Research article

FET PET provides adjunctive value to FDG PET in distinction of spinal cord tumors

Penghao Liu [a,1], Jing Huang [b,1], Wanru Duan [a,1], Tianbin Song [b], Jiyuan Wang [b], Can Zhang [a], Yueqi Du [a], Ye Chen [a], Renkui Fu [a], Jie Lu [b,**], Zan Chen [a,*]

[a] Department of Neurosurgery, Xuanwu Hospital, Capital Medical University, Beijing, 100053, China
[b] Department of Radiology and Nuclear Medicine, Xuanwu Hospital, Capital Medical University, Beijing, 100053, China

A R T I C L E   I N F O

A B S T R A C T

Objective: This study aimed to compare the diagnostic efficacy of O-(2-^{18}F-fluoroethyl)-L-tyrosine (^{18}F-FET) PET and 2-deoxy-2-[^{18}F]fluoro-D-deoxyglucose (^{18}F-FDG) PET for spinal cord lesions.
Materials and methods: Paired preoperative ^{18}F-FDG PET/MRI and ^{18}F-FET PET/MRI scans were conducted on patients with suspected spinal cord tumors. Clinical manifestations and PET performance, including SUVmean, SUVmax, TBRmean, TBRmax, metabolic tumor volume (MTV), and total lesion metabolism (TLM), and tumor volume, were compared using group analysis and receiver operating characteristic (ROC) curves.
Results: Thirty-five patients were categorized into three groups based on their pathological diagnosis: high-grade tumors (HGTs, n = 6), low-grade tumors (LGTs, n = 19), and non-tumor diseases (NTDs, n = 10). The background SUVmean of ^{18}F-FET PET was significantly lower than that of ^{18}F-FDG PET (p < 0.0001), while the delineated tumor volumes showed no significant difference (p > 0.05). The mass SUVmean, SUVmax, MTV, and TLM values of both ^{18}F-FDG PET and ^{18}F-FET PET were statistically different between HGTs and LGTs (p < 0.05). Similarly, the mass SUVmax, TBRmax, MTV, and TLM values of both ^{18}F-FDG PET and ^{18}F-FET PET, as well as the mass SUVmean of ^{18}F-FET PET, exhibited statistical differences between HGTs and NTDs (p < 0.05). But none were able to distinguish LGTs and NTDs (p > 0.05). Notably, ^{18}F-FET PET provided valuable supporting diagnostic evidence in 1 case of mixed neuronal-glial tumor (MNGT) and 2 cases of intramedullary inflammatory lesions. Optimal cut-off values of all measured parameters for distinguishing tumors and NTDs were determined through ROC analysis.
Conclusion: ^{18}F-FET PET presented comparable diagnostic performance to ^{18}F-FDG PET in differentiating HGTs, LGTs, and NTDs, but exhibited particular utility in MNGT and inflammatory lesions.

* Corresponding author. Department of Neurosurgery Xuanwu Hospital, Capital Medical University 45 Changchun Street, Xicheng District, Beijing, China.
** Corresponding author. Department of Radiology and Nuclear Medicine, Xuanwu Hospital, Capital Medical University 45 Changchun Street, Xicheng District, Beijing, China.
E-mail addresses: liuph14@hotmail.com (P. Liu), sainthj@126.com (J. Huang), duanwanru@xwhosp.org (W. Duan), Songtb_1984@163.com (T. Song), wjiyuan2023@163.com (J. Wang), duyueqi@163.com (Y. Du), chenyeah58@gmail.com (Y. Chen), renkui.fu@foxmail.com (R. Fu), imaginglu@hotmail.com (J. Lu), chenzan66@163.com (Z. Chen).
[1] These authors contributed equally to this work.

1. Introduction

Abbreviation list

AA   Anaplastic astrocytoma
AAD   Atlantoaxial dislocation
ACDF   Anterior cervical discectomy and fusion
AUC   Area under the ROC curve
CNS   Central nervous system
DMG   Diffuse midline glioma
DOPA   Dihydroxyphenylalanine
EPN   Ependymoma
^{18}F-FET   O-(2-^{18}F-fluoroethyl)-L-tyrosine
^{18}F-FDG   2-deoxy-2-[^{18}F]fluoro-D-deoxyglucose
GG   Ganglioglioma
GN   Granuloma
HGTs   High-grade tumors
IDP   Intervertebral disc protrusions
LGTs   Low-grade tumors
MET   Methionine
MNGT   Mixed neuronal-glial tumor
MRI   Magnetic Resonance Imaging
MTV   Metabolic tumor volume
NTDs   Non-tumor diseases
OSEM   Ordered-subset expectation-maximization
PCDF   Posterior cervical discectomy and fusion
PCR   Polymerase chain reaction
PET   Positron emission tomography
ROC: Receiver operating characteristic
ROIs   Regions of interest
SD   Standard deviation
SUVmax   Maximum standardized uptake value
SUVmean   Mean standardized uptake value
TBRmax   Maximum target/background ratio
TBRmean   Mean target/background ratio
TLM   Total lesion metabolism

Spinal cord tumors are a relatively rare occurrence, constituting approximately 3 % of all primary central nervous system (CNS) tumors [1]. Complete resection of intramedullary tumors is challenging due to the dense distribution of neurons and nerve fibers along the spinal cord, leading to a high risk of causing additional neurological damage or tumor recurrence [2].

Magnetic Resonance Imaging (MRI) of the spinal cord can precisely determine the location and morphology of spinal cord lesions. Positron emission tomography (PET) provides a superior demonstration of the biological functions, including metabolic characteristics and tumor perfusion. This technique enhances diagnostic efficacy and enables more accurate prediction of disease prognosis [3]. Currently, the most commonly used PET tracer is 2-deoxy-2-[^{18}F]fluoro-D-deoxyglucose (^{18}F-FDG), which shows high uptake in various CNS tumors and exhibits a strong correlation with their prognosis [3]. However, the specificity of ^{18}F-FDG PET is affected by the additional uptake of inflammatory lesions and the presence of high background signals in normal CNS tissues [4–7].

Recent studies in CNS PET imaging have focused on amino acids and amino acid analogs as promising tracers [8–10]. O-(2-^{18}F-fluoroethyl)-L-tyrosine (^{18}F-FET) PET is an analog of tyrosine that exhibits an exceptionally high metabolic rate in CNS tumors and a low background signal. Hence, it serves as a potential PET tracer for spinal cord tumors [10]. Nevertheless, there is limited experience in using ^{18}F-FET PET to assess spinal cord involvement in clinical practice, and there is a scarcity of comparative studies between ^{18}F-FET PET and ^{18}F-FDG PET for spinal cord lesions [11,12]. Therefore, this study retrospectively compared the diagnostic efficacy of ^{18}F-FET PET and ^{18}F-FDG PET in patients with suspected spinal cord tumors.

2. Materials and methods

2.1. Patients

This retrospective study analyzed a consecutive cohort of patients with suspected intramedullary tumors in our center, who

underwent both ^{18}F-FDG PET/MRI and ^{18}F-FET PET/MRI scans before surgery, from January 2022 to June 2023. One patient underwent ^{18}F-FDG PET/CT and ^{18}F-FET PET/CT instead due to claustrophobia. Patients who suffered from intervertebral disc protrusions and atlantoaxial dislocation with abnormal intramedullary signals on MRI were also included. All of the enrolled patients presented abnormal signals within the spinal cord on MRI, with an ECOG performance score below 3. They exhibited no allergic reactions to the ^{18}F-FDG and ^{18}F-FET tracers. Intramedullary lesion resections were performed when tumors were suspected, and tissue samples were tested and analyzed by experienced pathologists. Patients with intervertebral disc protrusions (IDP) were given the options of observation or surgery. Subsequently, the patient's clinical presentation, pathological diagnosis, and ^{18}F-FDG PET/MRI and ^{18}F-FET PET/MRI images were collected. Written Informed Consent Forms for both surgery and research were obtained according to the Declaration of Helsinki from all patients. This study received approval from the Research Ethics Committee of Xuanwu Hospital of Capital Medical University.

2.2. ^{18}F-FET PET and ^{18}F-FDG PET image acquisition

Preoperative ^{18}F-FDG PET and ^{18}F-FET PET scans were conducted on separate days within a one-week timeframe. Patients were instructed to refrain from consuming food and water for 12 h prior to the ^{18}F-FDG PET examination, and their blood glucose levels were required to be below 6 mmol/L on the examination day. Prior to the ^{18}F-FET PET scan, patients were instructed to adhere to a low-protein diet for 24 h and maintain fasting from food and water for 6 h preceding the examination. ^{18}F-FET was produced as described previously [13]. PET and MR data were acquired simultaneously using a 3-T hybrid PET/MR scanner (uPMR790, UIH, Shanghai, China) either 40–60 min after intravenous administration of 3.7 MBq/kg of ^{18}F-FDG tracer or 20 min after intravenous injection of 185 ± 10 % MBq of ^{18}F-FET tracer [14]. Time of flight (TOF) and ordered-subset expectation-maximization (OSEM) techniques were applied for image reconstruction.

2.3. Analysis of PET imaging

Two senior nuclear medicine physicians (Song T. and Huang J.) independently conducted qualitative visual analysis. In cases of disagreement, a third nuclear medicine specialist (Lu J.) was consulted. PET attenuation correction maps were generated from MR images after image segmentation as previously reported [15]. PET/MR images were quantitatively analyzed using the uWS-MI workstation (UIH, Shanghai, China) to identify abnormal signals within the spinal cord and measure the metabolic characteristics of the lesions in both ^{18}F-FDG PET and ^{18}F-FET PET scans. Regions of interest (ROIs) were chosen within the intramedullary lesions, and their quantitative measurements included the mean standardized uptake value (SUVmean), maximum standardized uptake value (SUVmax), metabolic tumor volume (MTV), and total lesion metablism (TLM, $TLM = MTV \times SUVmean$) values. The segment of medulla adjacent to the 7th cervical (C7) vertebrae was chosen as the background ROI. If lesions involved C7, the nearest lesion-free segment below was selected as the background ROI. The background SUVmean was quantitatively measured, and both the mean target/background ratio (TBRmean) and the maximum target/background ratio (TBRmax) were calculated. The impacts of ^{18}F-FDG PET and ^{18}F-FET PET on clinical decision-making were independently evaluated by two surgeons (Liu P. and Duan W.). In cases of disagreements, a third surgeon (Chen Z.) was consulted.

2.4. Pathology

Patients with suspected intramedullary tumors underwent surgeries after comprehensive preoperative analysis, and the obtained samples were collected for pathological examination. The samples were immersed in 4 % paraformaldehyde for 48 h to fix, which was followed by dehydration using alcohol and xylene gradients (concentrations of 75 %, 85 %, 90 %, and 100 %). The tissues were then embedded in paraffin wax, sectioned on a microtome at a thickness of 4 μm, and subsequently subjected to H&E staining and immunohistochemical staining. Patients diagnosed with gliomas underwent additional molecular pathological examinations, including polymerase chain reaction (PCR) and Sanger sequencing. Pathological diagnosis was made by integrating the histology and molecular pathological results.

2.5. Statistical analysis

The differences between groups were compared using a non-parametric test (Mann-Whitney test) in this study. Statistical analysis was conducted using SPSS (version 26.0, IBM SPSS Statistics software). Graphs were generated using GraphPad Prism software (version 8, GraphPad Software). Receiver operating characteristic (ROC) analysis was conducted using MedCalc software (version 22.002, MedCalc Software Ltd., Ostend, Belgium) to calculate the area under the ROC curve (AUC) and its standard deviation (SD). Differences between the ROC curves of ^{18}F-FDG PET and ^{18}F-FET PET were assessed using a two-tailed univariate Z-score test. Statistical significance was defined as a two-tailed p-value less than 0.05.

3. Results

3.1. Patient characteristics

Thirty-five patients (mean age 58 years, 13–75 years, 45.7 % male) underwent paired ^{18}F-FDG PET/MRI and ^{18}F-FET PET/MRI

examinations prior to surgery (see Table 1). The lesions were primarily located in the cervical medulla (n = 26, 74.3 %), with additional involvement in the thoracic medulla (n = 15, 42.9 %) and lumbar medulla (n = 2, 5.7 %) (see Table 1). Six patients (17.1 %) were diagnosed with high-grade tumors (HGTs) based on pathology and clinical presentation. This group included five cases of H3K27M-mutant diffuse midline glioma (DMG) of WHO grade IV and one case of anaplastic astrocytoma (AA) of WHO grade III. Nineteen patients (54.3 %) were diagnosed with low-grade tumors (LGTs), which included various tumor types: nine cases of ependymoma (EPN) of WHO grade II, one case of astrocytoma of WHO grade II, one case of mixed neuronal-glial tumor (MNGT) of WHO grade II, one case of MNGT/ganglioglioma (GG) of WHO grade I, one case of schwannoma of WHO grade I, one case of hemangioblastoma of WHO grade I, and five cases of vascular malformation. Ten patients (28.6 %) were diagnosed with non-tumor diseases (NTDs), which included five cases of IDP, three cases of gliosis, one case of granuloma, and one case of atlantoaxial dislocation (AAD) (see Supplemientary Table S1).

The average spinal background SUVmean on ^{18}F-FET PET was 0.54 (standard deviation, SD = 0.19), which was significantly lower compared to ^{18}F-FDG PET (mean = 1.17, SD = 0.24, p < 0.0001). In terms of impacts on clinical decision-making, ^{18}F-FDG PET was rated as follows: A (influenced clinical management) in one case (2.9 %), B (added important clinical information) in twenty-nine cases (82.9 %), and C (supported clinical decision) in five cases (14.3 %). In contrast, for ^{18}F-FET PET, three cases (8.6 %) were rated as A, twenty-four cases (68.6 %) as B, and eight cases (22.9 %) as C (see Table 1).

Among the patients, limb numbness was observed in ten cases, limb pain in four cases, limb weakness in four cases, and seventeen patients exhibited a combination of these three symptoms. Additionally, three patients experienced urinary or fecal disorders. Among the patients, twenty-eight underwent intramedullary lesion resection, two underwent anterior cervical discectomy and fusion (ACDF), one underwent posterior cervical discectomy and fusion (PCDF), one underwent intramedullary lesion resection combined with ACDF, and three patients were managed conservatively (see Supplementary Table S1).

3.2. ^{18}F-FDG PET and ^{18}F-FET PET measurement

Table 2 presents the values of the mass SUVmean, SUVmax, TBRmean, TBRmax, MTV, TLM, tumor volume, and the spinal background SUVmean for all patients in the preoperative ^{18}F-FDG PET and ^{18}F-FET PET. There was no statistically significant difference in tumor volume between the ^{18}F-FDG PET and ^{18}F-FET PET groups (p = 0.78).

No statistically significant differences were found in the background SUVmean of ^{18}F-FDG PET and ^{18}F-FET PET among the HGT, LGT, and NTD groups (p = 0.27, see Table 3). The SUVmean, SUVmax, TBRmax, MTV, and TLM values of the mass in ^{18}F-FDG PET and ^{18}F-FET PET showed statistically significant differences among the three groups (p < 0.05). Conversely, the TBRmean values of the mass in ^{18}F-FDG PET and ^{18}F-FET PET did not show statistically significant differences between the groups (p = 0.096).

Table 1
Basic characteristics of the patients with simultaneous^{18}F-FDG PET and^{18}F-FET PET.

Characteristic	Data
Total (n)	35
Age (median/range)	58/13-75
Sex	
Male	16 (45.7 %)
Female	19 (54.3 %)
Diagnosis	
HGT	6 (17.1 %)
LGT	19 (54.3 %)
NTD	10 (28.6 %)
Involved segments	
Cervical	26 (74.3 %)
Thoracic	15 (42.9 %)
Lumbar	2 (5.7 %)
Spinal background SUVmean	
FDG-PET (mean/SD)	1.17/0.24
FET-PET (mean/SD)	0.54/0.19
Impact of FDG-PET[a]	
A	1 (2.9 %)
B	29 (82.9 %)
C	5 (14.3 %)
Impact of FET-PET[a]	
A	3 (8.6 %)
B	24 (68.6 %)
C	8 (22.9 %)

Abbreviation: HGT: high-grade tumor, LGT: low-grade tumor, NTD: non-tumor diseases.

[a] Impact of PET: A: Influenced clinical management, B: Added important clinical information, C: Supported clinical decision.

Table 2
Parameter measurement of[18]F-FDG PET and[18]F-FET-PET on patients with the suspected diagnosis of spinal cord tumors.

Number	Diagnosis	WHO grading	Location	^{18}F-FDG-PET								^{18}F-FET-PET							
				Background SUVmean	SUVmean	SUVmax	TBRmean	TBRmax	MTV	TLM	Volume/cm³	Background SUVmean	SUVmean	SUVmax	TBRmean	TBRmax	MTV	TLM	Volume/cm³
1	DMG	IV	T11-L1	1.31	2.43	13.36	1.85	10.20	7.58	13.91	4.7	1.07	2.18	4.94	2.04	4.62	3.06	7.23	4.6
2	DMG	IV	C4–C6	1.33	3.66	7.94	2.75	5.97	4.26	8.16	2.2	0.56	1.84	2.52	3.29	4.50	8.97	10.24	2.1
3	DMG	IV	T8-T10	1.21	2.96	6.15	2.45	5.08	4.16	6.05	4.9	0.85	1.29	1.61	1.52	1.89	1.93	2.4	4.8
4	DMG	IV	T11-T12	0.84	3.33	5.99	3.96	7.13	4.77	8.3	3.8	0.77	1.55	2.12	2.01	2.75	1.68	3.5	3.5
5	DMG	IV	C1–C3	1.19	1.24	1.67	1.04	1.40	2.8	3.59	2.4	0.65	0.94	1.87	1.45	2.88	2.92	2.6	2.5
6	AA	III	T3-T4	0.93	3.25	10.96	3.49	11.78	7.14	11.48	18.2	0.59	1.98	3.88	3.36	6.58	2.75	5.06	19.1
7	EPN	II	C3–C5	1.34	2.39	7.83	1.78	5.84	3.69	6.61	1.1	0.46	1.46	1.69	3.17	3.67	1.1	2.53	0.8
8	EPN	II	C4	1.54	2.93	6.31	1.90	4.10	3.04	5.7	1.8	0.67	0.86	0.94	1.28	1.40	0.59	1.68	1.6
9	EPN	II	C6-T1	1.25	1.59	2.29	1.27	1.83	2.86	3.03	2.4	0.51	1.01	1.33	1.98	2.61	0.89	0.97	2.2
10	EPN	II	C7-T1	1.28	1.27	1.32	0.99	1.03	NA	NA	NA	0.31	0.30	0.32	0.97	1.03	NA	NA	NA
11	EPN	II	C4-5	0.44	3.75	8.64	8.52	19.64	9.21	9.76	1	0.52	1.54	2.82	2.96	5.42	2.97	3.02	1.1
12	EPN	II	T12	0.89	1	1.63	1.12	1.83	1.48	1.53	1.5	0.25	0.53	0.67	2.12	2.68	0.91	0.97	1.3
13	EPN	II	C4-5	0.88	1.78	2.75	2.02	3.13	2.97	3.02	4.2	0.41	0.42	0.48	1.02	1.17	0.42	0.47	4.4
14	EPN	II	T11-L1	1.06	1.89	2.77	1.78	2.61	2.37	3.81	1.3	0.27	0.58	0.79	2.15	2.93	0.6	1.06	1.3
15	EPN	II	C6–C7	1.28	2.25	3.49	1.76	2.73	2.37	2.98	1.9	0.49	0.91	1.06	1.86	2.16	0.72	1.59	1.8
16	Astrocytoma	II	C1–C3	1.3	1.58	3.05	1.22	2.35	2.19	5.42	3.8	0.66	1.85	2.91	2.80	4.41	2.07	5.09	3.9
17	MNGT	II	C4-T4	1.48	2.84	15.51	1.92	10.48	6.86	12	2.3	0.69	1.14	2.26	1.65	3.28	1.19	2.56	2.1
18	MNGT/GG	I	T4-T9	1.06	1.43	2.18	1.35	2.06	2.36	4.53	8.8	0.72	1.26	1.96	1.75	2.72	1.79	3.81	10.4
19	Schwannoma	I	T10	1.24	1.3	1.99	1.05	1.60	1.74	1.96	1.1	0.32	0.57	0.88	1.78	2.75	1.02	1.08	1
20	HGB	I	C2-T2	1.21	1.95	2.29	1.61	1.89	2.69	2.98	3.4	0.6	0.9	0.99	1.50	1.65	0.67	0.74	3.3
21	VM	–	C6–C7	1.29	1.95	3.01	1.51	2.33	3.69	3.75	1.7	0.65	1.12	2.24	1.72	3.45	2.87	2.95	1.4
22	VM	–	T3	1.38	1.9	2.31	1.38	1.67	2.69	2.76	0.5	0.57	0.57	0.75	1.00	1.32	0.71	0.75	0.5
23	VM	–	C5-T1	1.03	1.18	1.22	1.15	1.18	1.19	1.32	1.1	0.35	0.37	0.41	1.06	1.17	0.43	0.52	1
24	VM	–	C3–C4	1.41	2.78	3.96	1.97	2.81	2.7	6.27	2.1	0.62	1.28	1.96	2.06	3.16	1.42	3.44	1.9
25	VM	–	C5-T2	1.37	1.51	2.61	1.10	1.91	1.28	2.89	4.3	0.82	1.64	2.31	2.00	2.82	1.31	3.05	4.3
26	GN	–	C5–C6	1.38	4.45	8.51	3.22	6.17	4.33	8.54	NA	0.71	1.51	1.91	2.13	2.69	1.08	2.74	NA
27	Gliosis	–	C1–C4	1.6	3.55	7.66	2.22	4.79	5.87	6.98	NA	0.46	1.53	2.29	3.33	4.98	2.11	2.59	NA
28	Gliosis	–	C6–C7	1.02	1.35	2.34	1.32	2.29	2.87	2.98	NA	0.25	0.42	0.56	1.68	2.24	0.43	0.48	NA
29	Gliosis	–	C5–C6	1.04	1.77	2.47	1.70	2.38	1.86	2.03	NA	0.41	0.58	0.65	1.41	1.59	1.35	1.43	NA
30	AAD	–	C1-3	0.98	0.95	1.67	0.97	1.70	1.68	1.99	NA	0.43	0.52	0.74	1.21	1.72	3	1.31	NA
31	IDP	–	C4–C5	1.16	1.15	1.39	0.99	1.20	1.29	1.32	NA	0.34	0.47	0.67	1.38	1.97	0.52	0.57	NA
32	IDP	–	C2–C3	1.33	1.51	1.88	1.14	1.41	1.49	3.34	NA	0.77	1.44	1.85	1.87	2.40	0.92	2.18	NA
33	IDP	–	C2-5	1.02	2.04	2.89	2.00	2.83	3.68	4.02	NA	0.35	0.35	0.39	1.00	1.11	0.27	0.33	NA
34	IDP	–	C6	1.14	1.7	2.79	1.49	2.45	2.35	2.76	NA	0.35	0.6	0.83	1.71	2.37	1.13	1.19	NA
35	IDP	–	C5-6	0.68	1.24	1.45	1.82	2.13	2.12	2.87	NA	0.4	0.57	0.74	1.43	1.85	1.21	1.36	NA

Abbreviation: AAD: Atlantoaxial dislocation, ACDF: Anterior cervical discectomy and fusion, DMG: AA: anaplastic astrocytoma, Diffuse midline glioma H3 K27 M mutated, EPN: ependymoma, GG: ganglioglioma, GN: granuloma, HGB: hemangioblastoma, IDP: Intervertebral disc protrusion, MNGT: Mixed neuronal-glial tumors, MTV: metabolic tumor volume, PCDF: Posterior cervical discectomy and fusion, SUV: standardized uptake value, SUVmax: maximum standardized uptake value, SUVmean: mean standardized uptake value, TBR: target/background ratio, TBRmean: mean target/background ratio, TBRmax: maximum target/background ratio, TLM: total lesion metabolism, VM: vascular malformation.

3.3. ^{18}F-FDG PET and ^{18}F-FET PET in differential diagnosis between high-grade tumors, low-grade tumors and non-tumor diseases

A comparison was conducted between the HGT, LGT, and NTD groups for the parameters of ^{18}F-FDG PET and ^{18}F-FET PET, respectively (see Fig. 1). The mass SUVmean, SUVsmax, TBRmax, MTV, and TLM values of ^{18}F-FDG PET and ^{18}F-FET PET were statistically significantly different ($p < 0.05$) between the HGT and LGT groups. And significant differences ($p < 0.05$) were found in the mass SUVmax, TBRmax, MTV, and TLM values of ^{18}F-FDG PET and ^{18}F-FET PET, as well as the mass SUVmean of ^{18}F-FET PET, between the HGT and NTD groups. The mass TBRmean values of ^{18}F-FDG PET and ^{18}F-FET PET were indistinguishable among HGT, LGT and NTD groups. And none of the parameters showed distinguishable differences between the LGT and NTD groups.

3.4. Diagnostic efficacy of ^{18}F-FDG PET and ^{18}F-FET PET in tumors and non-tumor diseases

We conducted ROC analysis for each measured parameter of ^{18}F-FDG PET and ^{18}F-FET PET in both tumor and NTD groups. The optimal cut-off values for each parameter (SUVmean, SUVmax, TBRmean, TBRmax, MTV, and TLM) in differentiating the two groups were calculated (see Fig. 2). In all parameters ^{18}F-FET PET showed non-inferior diagnostic performances to ^{18}F-FDG PET ($p > 0.05$). And ^{18}F-FET PET showed tendency of better performance than ^{18}F-FDG PET in terms of SUVmean, SUVmax, TBRmean, and TBRmax, though not statistically significant. Among all parameters, SUVmax was the most promising candidate for distinguishing tumors and NTDs, with the optimal cut-off value of 2.54 (AUC = 0.63, 95 % CI 0.42–0.83, sensitivity = 0.64, 95 % CI 0.45–0.80, specificity = 0.60, 95 % CI 0.31–0.83) in ^{18}F-FDG PET, and 0.86 (AUC = 0.72, 95 % CI 0.53–0.90, sensitivity = 0.76, 95 % CI 0.57–0.88, specificity = 0.70, 95 % CI 0.40–0.89) in ^{18}F-FET PET.

In Case 17, ^{18}F-FDG PET revealed high uptake with an SUVmax of 15.51 and TBRmax of 10.48, indicative of a HGT. However, ^{18}F-FET PET exhibited low uptake with an SUVmax of 1.14 and TBRmax of 1.65, contradicting the previous diagnosis. The pathological examination confirmed the diagnosis of a MNGT classified as WHO grade II (see Supplementary Fig. S1). The pathological diagnoses for Case 26 and Case 27 were GN and gliosis, respectively. However, the MRI findings and high uptake of ^{18}F-FDG PET indicated the possibility of HGTs. The ^{18}F-FET PET of Case 26 exhibited low uptake of with an SUVmax of 1.91 and TBRmax of 2.69 (see Supplementary Fig. S2). And the ^{18}F-FET PET of Case 27 exhibited moderate uptake with an SUVmax of 2.29 and TBRmax of 4.98 [16].

4. Discussion

This retrospective study analyzed the imaging presentations of 35 patients with suspected intramedullary tumors, including HGTs (n = 6), LGTs (n = 19), and NTDs (n = 10) using ^{18}F-FDG PET and ^{18}F-FET PET. Our primary focus was on quantifying and calculating various parameters such as the mass SUVmean, SUVmax, TBRmean, TBRmax, MTV, TLM values, and tumor volumes. It was observed that the spinal cord background SUVmean values were lower in ^{18}F-FET PET compared to ^{18}F-FDG PET. Importantly, the diagnostic performance of ^{18}F-FET PET was comparable to that of ^{18}F-FDG PET across the HGT, LGT, and NTD groups. A ^{18}F-FET PET exhibited certain advantages in identifying specific low-grade tumors and inflammatory lesions as shown below by cases.

Five out of the six patients who were assigned to the HGT group were diagnosed as H3K27M-mutant DMGs. According to the 2016 WHO Classification of CNS Tumors, H3K27M-mutant DMGs are categorized as grade IV and predominantly occur in the cerebellum, brainstem, and spinal cord, with a dismal prognosis [17,18]. In pediatric patients, the prognosis of DMGs has been correlated with ^{18}F-FDG uptake, which is currently the most commonly used PET tracer for these tumors [19]. However, there has been growing interest in the use of amino acid PET tracers on CNS tumors, including ^{18}F-FET, ^{18}F-dihydroxyphenylalanine (DOPA), and ^{11}C-methionine (MET) [11,12,20,21]. Nevertheless, most studies have focused on brain tumors, and limited evidence exists regarding spinal cord tumors. In a retrospective study evaluating the performance of ^{18}F-FDG PET and ^{11}C-MET PET in intramedullary lesions, the SUVmax values of both tracers were effective in delineating HGTs but not LGTs or NTDs [22]. Notably, ^{18}F-FET, with its longer half-life compared to ^{11}C-MET, exhibited superior performances in distinguishing inflammatory diseases [23]. Tscherpel C. et al. [11] reported the increased ^{18}F-FET PET uptake (TBRmax≥2.5 and/or TBRmean≥1.9) in all patients with high-grade gliomas and in nearly half of those with low-grade gliomas involving the brainstem and spinal cord.

In this study, both ^{18}F-FDG PET and ^{18}F-FET PET demonstrated increased uptake in the HGT group. The mass SUVmean, SUVmax,

Table 3
Mean and standard deviation of ^{18}F-FDG-PET and ^{18}F-FET-PET parameters.

Parameters/mean (SD)	HGT		LGT		NTD		P value
	^{18}F-FDG-PET	^{18}F-FET-PET	^{18}F-FDG-PET	^{18}F-FET-PET	^{18}F-FDG-PET	^{18}F-FET-PET	
Background SUVmean	1.14 (0.20)	0.75 (0.19)	1.20 (0.26)	0.52 (0.17)	1.14 (0.25)	0.45 (0.16)	0.27
SUVmean	2.81 (0.87)	1.63 (0.46)	1.96 (0.71)	0.96 (0.46)	1.97 (1.14)	0.80 (0.49)	0.044
SUVmax	7.68 (4.11)	2.82 (1.31)	3.96 (3.48)	1.41 (0.83)	3.31 (2.58)	1.06 (0.68)	0.027
TBRmean	2.59 (1.07)	2.28 (0.85)	1.86 (1.65)	1.83 (0.64)	1.69 (0.69)	1.71 (0.65)	0.096
TBRmax	6.92 (3.72)	3.87 (1.70)	3.74 (4.41)	2.62 (1.17)	2.73 (1.56)	2.29 (1.05)	0.027
MTV	5.12 (1.86)	3.55 (2.71)	3.08 (1.98)	1.20 (0.77)	2.75 (1.46)	1.20 (0.82)	0.0066
TLM	8.58 (3.70)	5.17 (3.07)	4.46 (2.82)	2.02 (1.34)	3.68 (2.31)	1.42 (0.85)	0.0086

Abbreviation: HGT: high-grade tumor, LGT: low-grade tumor, MTV: metabolic tumor volume, NTD: non-tumor diseases, SUV: standardized uptake value, SUVmax: maximum standardized uptake value, SUVmean: mean standardized uptake value, TBR: target/background ratio, TBRmax: maximum target/background ratio, TBRmean: mean target/background ratio, TLM: total lesion metabolism.
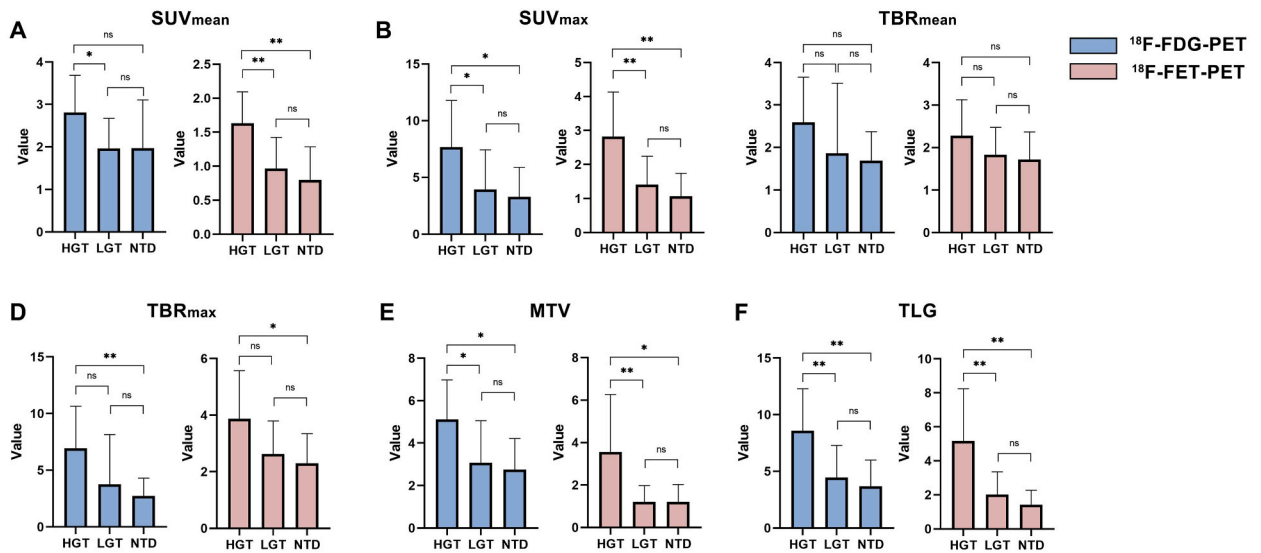
Fig. 1. Measured ^{18}F-FDG PET and ^{18}F-FET PET parameters in HGT, LGT, and NTD groups. Comparison of A. SUVmean, B. SUVmax, C. TBRmean, D. TBRmax, E. MTV, and F. TLM between the HGT, LGT, and NTD groups.
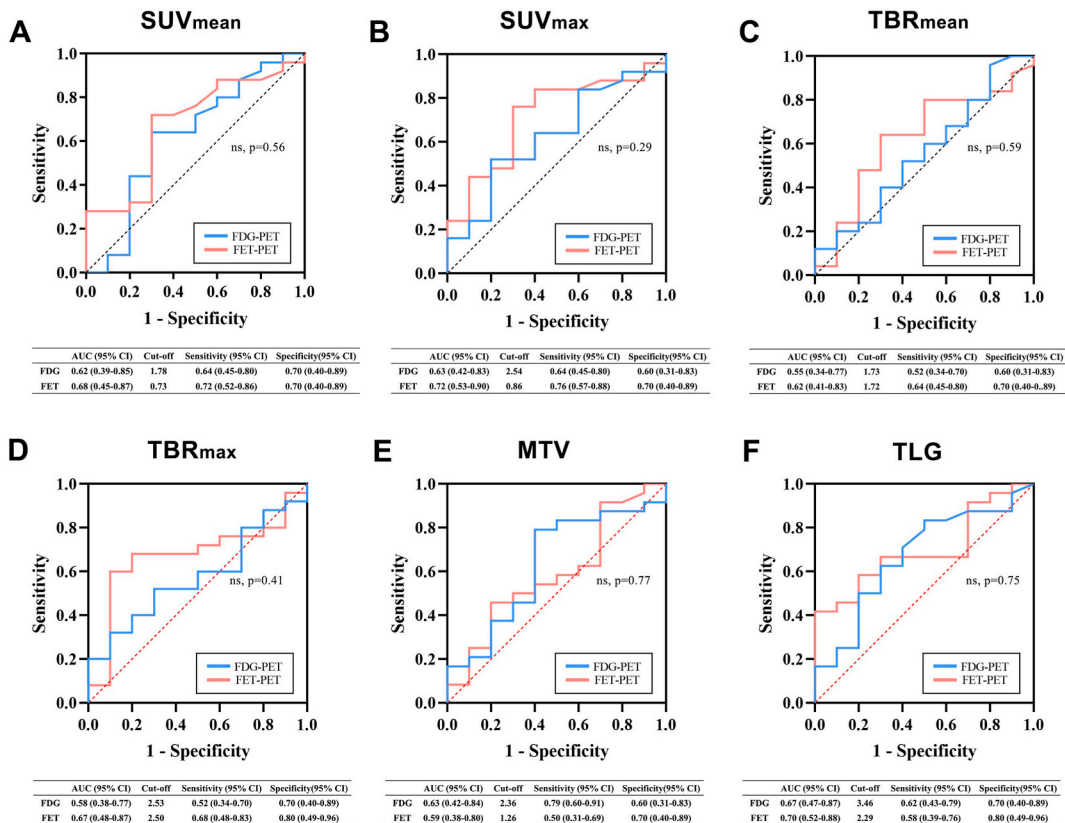

Fig. 2. ROC curves of the measured parameters of ^{18}F-FDG PET and ^{18}F-FET PET in differentiating tumors and non-tumor diseases. ROC curve analysis of A. SUVmean, B. SUVmax, C. TBRmean, D. TBRmax, E. MTV, F. TLM.

MTV, and TLM values obtained from ^{18}F-FDG PET and ^{18}F-FET PET proved to be valuable for distinguishing between HGTs and LGTs. To be noted, the use of MTV and TLM in relation to ^{18}F-FET PET has never been previously reported. In Case 5, the patient was admitted due to the progression of limb weakness and hypoesthesia two years after the surgical resection of an intramedullary

H3K27M-mutant DMG. Although spinal MRI did not reveal any apparent lesions, cervical hypermetabolic lesions were detected through ^{18}F-FDG PET and ^{18}F-FET PET. The lesion was surgically removed, and the pathology confirmed the diagnosis of recurrent H3K27M-mutant DMG. In this particular case, both ^{18}F-FDG PET and ^{18}F-FET PET proved advantageous in monitoring recurrent intramedullary tumors.

Distinguishing between low-grade and high-grade intramedullary tumors is crucial as it impacts the extent of surgical resection and subsequently influences the severity of iatrogenic injuries. In Case 17 with MNGT, although ^{18}F-FDG PET suggested suspicion of HGTs, while ^{18}F-FET PET provided contradicting evidences indicative of an LGT. Meyer P.T. et al. [24] once reported a case of intracranial MNGT classified as WHO grade I, with increased uptake on ^{18}F-FDG PET, potentially leading to confusion with HGTs. This case suggested the importance of utilizing ^{18}F-FET PET in differentiating intramedullary MNGTs from HGTs.

In Case 26 and Case 27, ^{18}F-FET PET revealed low to moderate uptake, aiding in their differentiation from HGTs. Glucose is the most commonly consumed energy within the body, and its uptake is elevated not only in tumors but also in certain inflammatory conditions, such as infection, inflammation, and arterial plaques when there is a substantial recruitment of macrophages [6,25,26]. Amino acid metabolism, on the other hand, is more specific to tumors, and therefore, ^{18}F-FET PET has a higher signal-to-background ratio [27]. Tumor cells require a large number of amino acids to support protein synthesis during proliferation and simultaneously upregulate the expression of cellular amino acid transporters [28]. Studies have demonstrated the superiority of ^{18}F-FET PET over ^{18}F-FDG PET in distinguishing inflammatory lesions from tumors, and provided additional information on pathophysiological processes such as radionecrosis, pseudoprogression, and tumor recurrence [16,29,]. Our study further confirmed the additional diagnostic value of ^{18}F-FET PET in differentiating tumors from inflammatory lesions when compared to ^{18}F-FDG PET.

Although ^{18}F-FDG PET and ^{18}F-FET PET have been in development for decades, there remains an absence of established quantitative evaluation criteria for CNS tumors. Most studies rely on qualitative visual analysis, with only a few obtaining differential cut-off values in small sample sizes [8–10,30,31]. Naito K. et al. [22] conducted an evaluation of intramedullary lesions using ^{18}F-FDG PET and identified a SULmax (SUVmax corrected for lean body mass) value of 4.0 as the optimal threshold for distinguishing HGTs from LGTs, achieving a sensitivity of 100 % and specificity of 91.70 %. Meyer P.T. et al. [32] found that the TBRmax value of 0.7 for ^{18}F-FDG PET in brain tumors was the best threshold for differentiating tumors from NTDs, with a sensitivity of 83.3 % and specificity of 62.5 %. Pauleit D. et al. [33] suggested an optimal TBRmean threshold of 1.6 for ^{18}F-FET PET in the diagnosis of brain tumors and NTDs, achieving a sensitivity of 92 % and specificity of 81 %. However, these thresholds did not bring satisfactory diagnostic efficacy in our cohort, which is likely due to the lack of comprehensive assessment of PET parameters and the small sample sizes in previous studies. In our study, we included commonly observed spinal cord lesions suspected as tumors and reported the mean values of the mass SUVmean, SUVmax, TBRmean, TBRmax, MTV, and TLM in ^{18}F-FDG PET and ^{18}F-FET PET. We conducted ROC analysis to determine the optimal cut-off values for these measured parameters in both ^{18}F-FDG PET and ^{18}F-FET PET, aiming to provide quantitative data for future research on PET imaging of spinal cord lesions.

This study has certain limitations, including its retrospective design and small sample sizes for each disease, which may introduce potential selection bias. Also, the geographic and demographic diversity of the patient population largely restricted the applicability of the conclusions. Hopefully, the research provided a general clinical scenario for the application of the ^{18}F-FET PET in spinal cord tumors and revealed the non-inferior diagnostic performances to traditional ^{18}F-FDG PET, with unique value in specific cases. A larger-size prospective study should be conducted with strict enrollment criteria and experimental design, focusing on intramedullary inflammatory diseases or tumor pseudo-progression.

5. Conclusions

This study represents the first direct comparison of paired ^{18}F-FDG PET and ^{18}F-FET PET imaging in spinal cord lesions. The spinal background SUVmean of ^{18}F-FET PET was lower, increasing its specificity in delineating spinal cord lesions. Overall, ^{18}F-FET PET shared comparable performances with ^{18}F-FDG PET in distinguishing HGTs, LGTs, and NTDs. Additionally, our study demonstrated that the previously unreported MTV and TLM of ^{18}F-FET PET were valuable in differentiating HGTs and LGTs, as well as HGTs and NTDs. We also described the adjunctive function of ^{18}F-FET PET in distinguishing individual cases of MNGT and inflammatory lesions. A comprehensive ROC analysis was performed to determine the optimal cut-off values for the measured parameters of ^{18}F-FDG PET and ^{18}F-FET PET, providing guidance on further quantitative analysis. Therefore, ^{18}F-FET PET is recommended for suspected spinal cord tumors, as it shows promising capability in differential diagnosis, which warrants further clinical validation.

Data availability statement

The datasets generated or analyzed during the study have not been deposited into a publicly available repository, and are included

in article and supplementary material.

CRediT authorship contribution statement

Penghao Liu: Writing – original draft, Formal analysis. **Jing Huang:** Formal analysis. **Wanru Duan:** Writing – review & editing, Writing – original draft, Funding acquisition. **Tianbin Song:** Methodology. **Jiyuan Wang:** Methodology. **Can Zhang:** Visualization, Software. **Yueqi Du:** Data curation. **Ye Chen:** Investigation. **Renkui Fu:** Investigation. **Jie Lu:** Writing – review & editing, Supervision, Funding acquisition, Data curation, Conceptualization. **Zan Chen:** Writing – review & editing, Writing – original draft, Supervision, Resources, Funding acquisition, Data curation, Conceptualization.

Declaration of competing interest

The authors declare that they have no known competing financial interests or personal relationships that could have appeared to influence the work reported in this paper.

Acknowledgments

None.

Appendix A. Supplementary data

Supplementary data to this article can be found online at https://doi.org/10.1016/j.heliyon.2024.e33353.

References

[1] Q.T. Ostrom, G. Cioffi, K. Waite, C. Kruchko, J.S. Barnholtz-Sloan, CBTRUS statistical report: primary brain and other central nervous system tumors diagnosed in the United States in 2014-2018, Neuro Oncol. 23 (2021) iii1–iii105.
[2] J.C. Furlan, J.R. Wilson, E.M. Massicotte, A. Sahgal, M.G. Fehlings, Recent advances and new discoveries in the pipeline of the treatment of primary spinal tumors and spinal metastases: a scoping review of registered clinical studies from 2000 to 2020, Neuro Oncol. 24 (2022) 1–13.
[3] N. Sandu, G. Pöpperl, M.E. Toubert, T. Spiriev, B. Arasho, M. Orabi, et al., Current molecular imaging of spinal tumors in clinical practice, Mol. Med. 17 (2011) 308–316.
[4] R.S. Rosen, L. Fayad, R.L. Wahl, Increased 18F-FDG uptake in degenerative disease of the spine: characterization with 18F-FDG PET/CT, J. Nucl. Med. 47 (2006) 1274–1280.
[5] C.G. Radu, C.J. Shu, S.M. Shelly, M.E. Phelps, O.N. Witte, Positron emission tomography with computed tomography imaging of neuroinflammation in experimental autoimmune encephalomyelitis, Proc. Natl. Acad. Sci. U. S. A. 104 (2007) 1937–1942.
[6] M. Ogawa, S. Nakamura, Y. Saito, M. Kosugi, Y. Magata, What can be seen by 18F-FDG PET in atherosclerosis imaging? The effect of foam cell formation on 18F-FDG uptake to macrophages in vitro, J. Nucl. Med. 53 (2012) 55–58.
[7] Y. Nakamoto, M. Tatsumi, D. Hammoud, C. Cohade, M.M. Osman, R.L. Wahl, Normal FDG distribution patterns in the head and neck: PET/CT evaluation, Radiology 234 (2005) 879–885.
[8] E.W. Lau, K.J. Drummond, R.E. Ware, E. Drummond, A. Hogg, G. Ryan, et al., Comparative PET study using F-18 FET and F-18 FDG for the evaluation of patients with suspected brain tumour, J. Clin. Neurosci. 17 (2010) 43–49.
[9] R. Pichler, A. Dunzinger, G. Wurm, J. Pichler, S. Weis, K. Nussbaumer, et al., Is there a place for FET PET in the initial evaluation of brain lesions with unknown significance? Eur. J. Nucl. Med. Mol. Imag. 37 (2010) 1521–1528.
[10] M. Plotkin, C. Blechschmidt, G. Auf, F. Nyuyki, L. Geworski, T. Denecke, et al., Comparison of F-18 FET-PET with F-18 FDG-PET for biopsy planning of non-contrast-enhancing gliomas, Eur. Radiol. 20 (2010) 2496–2502.
[11] C. Tscherpel, V. Dunkl, G. Ceccon, G. Stoffels, N. Judov, M. Rapp, et al., The use of O-(2-18F-fluoroethyl)-L-tyrosine PET in the diagnosis of gliomas located in the brainstem and spinal cord, Neuro Oncol. 19 (2017) 710–718.
[12] L. Marner, K. Nysom, A. Sehested, L. Borgwardt, R. Mathiasen, O.M. Henriksen, et al., Early postoperative (18)F-FET PET/MRI for pediatric brain and spinal cord tumors, J. Nucl. Med. 60 (2019) 1053–1058.
[13] K. Hamacher, H.H. Coenen, Efficient routine production of the 18F-labelled amino acid O-2-18F fluoroethyl-L-tyrosine, Appl. Radiat. Isot. 57 (2002) 853–856.
[14] S. Song, Y. Cheng, J. Ma, L. Wang, C. Dong, Y. Wei, et al., Simultaneous FET-PET and contrast-enhanced MRI based on hybrid PET/MR improves delineation of tumor spatial biodistribution in gliomas: a biopsy validation study, Eur. J. Nucl. Med. Mol. Imag. 47 (2020) 1458–1467.
[15] I. Mecheter, L. Alic, M. Abbod, A. Amira, J. Ji, MR image-based attenuation correction of brain PET imaging: review of literature on machine learning approaches for segmentation, J. Digit. Imag. 33 (2020) 1224–1241.
[16] P. Liu, J. Huang, J. Lu, Z. Chen, W. Duan, Postoperative spinal 18 F-FDG PET pseudoprogression mimicking malignancy, Clin. Nucl. Med. 48 (2023) 702–703.
[17] D.N. Louis, A. Perry, G. Reifenberger, A. von Deimling, D. Figarella-Branger, W.K. Cavenee, et al., The 2016 world health organization classification of tumors of the central nervous system: a summary, Acta Neuropathol. 131 (2016) 803–820.
[18] A. Mackay, A. Burford, D. Carvalho, E. Izquierdo, J. Fazal-Salom, K.R. Taylor, et al., Integrated molecular meta-analysis of 1,000 pediatric high-grade and diffuse intrinsic pontine glioma, Cancer Cell 32 (2017) 520–537.e525.
[19] K.A. Zukotynski, S. Vajapeyam, F.H. Fahey, M. Kocak, D. Brown, K.I. Ricci, et al., Correlation of (18)F-FDG PET and MRI apparent diffusion coefficient histogram metrics with survival in diffuse intrinsic pontine glioma: a report from the pediatric brain tumor consortium, J. Nucl. Med. 58 (2017) 1264–1269.
[20] C.L. Tinkle, E.C. Duncan, M. Doubrovin, Y. Han, Y. Li, H. Kim, et al., Evaluation of (11)C-methionine PET and anatomic MRI associations in diffuse intrinsic pontine glioma, J. Nucl. Med. 60 (2019) 312–319.
[21] G. Morana, D. Tortora, G. Bottoni, M. Puntoni, G. Piatelli, F. Garibotto, et al., Correlation of multimodal (18)F-DOPA PET and conventional MRI with treatment response and survival in children with diffuse intrinsic pontine gliomas, Theranostics 10 (2020) 11881–11891.
[22] K. Naito, T. Yamagata, J. Arima, A. Abe, N. Tsuyuguchi, K. Ohata, et al., Qualitative analysis of spinal intramedullary lesions using PET/CT, J. Neurosurg. Spine 23 (2015) 613–619.
[23] W.A. Weber, H.J. Wester, A.L. Grosu, M. Herz, B. Dzewas, H.J. Feldmann, et al., O-(2-[18F]fluoroethyl)-L-tyrosine and L-[methyl-11C]methionine uptake in brain tumours: initial results of a comparative study, Eur. J. Nucl. Med. 27 (2000) 542–549.

[24] P.T. Meyer, U. Spetzger, H.D. Mueller, T. Zeggel, O. Sabri, M. Schreckenberger, High F-18 FDG uptake in a low-grade supratentorial ganglioma: a positron emission tomography case report, Clin. Nucl. Med. 25 (2000) 694–697.

[25] W. Xuan, M.S. Lesniak, C.D. James, A.B. Heimberger, P. Chen, Context-dependent glioblastoma-macrophage/microglia symbiosis and associated mechanisms, Trends Immunol. 42 (2021) 280–292.

[26] E.J. Folco, Y. Sheikine, V.Z. Rocha, T. Christen, E. Shvartz, G.K. Sukhova, et al., Hypoxia but not inflammation augments glucose uptake in human macrophages: implications for imaging atherosclerosis with 18fluorine-labeled 2-deoxy-D-glucose positron emission tomography, J. Am. Coll. Cardiol. 58 (2011) 603–614.

[27] N.L. Albert, N. Galldiks, B.M. Ellingson, M.J. van den Bent, S.M. Chang, F. Cicone, et al., PET-based response assessment criteria for diffuse gliomas (PET RANO 1.0): a report of the RANO group, Lancet Oncol. 25 (2024) e29–e41.

[28] M. Harat, J. Rakowska, M. Harat, T. Szylberg, J. Furtak, I. Miechowicz, et al., Combining amino acid PET and MRI imaging increases accuracy to define malignant areas in adult glioma, Nat. Commun. 14 (2023) 4572.

[29] N. Spaeth, M.T. Wyss, B. Weber, S. Scheidegger, A. Lutz, J. Verwey, et al., Uptake of 18F-fluorocholine, 18F-fluoroethyl-L-tyrosine, and 18F-FDG in acute cerebral radiation injury in the rat: implications for separation of radiation necrosis from tumor recurrence, J. Nucl. Med. 45 (2004) 1931–1938.

[30] D. Pauleit, G. Stoffels, A. Bachofner, F.W. Floeth, M. Sabel, H. Herzog, et al., Comparison of (18)F-FET and (18)F-FDG PET in brain tumors, Nucl. Med. Biol. 36 (2009) 779–787.

[31] V. Dunet, A. Pomoni, A. Hottinger, M. Nicod-Lalonde, J.O. Prior, Performance of 18F-FET versus 18F-FDG-PET for the diagnosis and grading of brain tumors: systematic review and meta-analysis, Neuro Oncol. 18 (2016) 426–434.

[32] P.T. Meyer, M. Schreckenberger, U. Spetzger, G.F. Meyer, O. Sabri, K.S. Setani, et al., Comparison of visual and ROI-based brain tumour grading using 18F-FDG PET: ROC analyses, Eur. J. Nucl. Med. 28 (2001) 165–174.

[33] D. Pauleit, F. Floeth, K. Hamacher, M.J. Riemenschneider, G. Reifenberger, H.W. Müller, et al., O-(2-[18F]fluoroethyl)-L-tyrosine PET combined with MRI improves the diagnostic assessment of cerebral gliomas, Brain 128 (2005) 678–687.